

De Novo Design of Ln(III) Coiled Coils for Imaging Applications

Matthew R. Berwick,[†] David J. Lewis,[†] Andrew W. Jones,[‡] Rosemary A. Parslow,[‡] Timothy R. Dafforn,[‡] Helen J. Cooper,[‡] John Wilkie,[†] Zoe Pikramenou,[†] Melanie M. Britton,[†] and Anna F. A. Peacock^{*†}

[†]School of Chemistry and [‡]School of Biosciences, University of Birmingham, Edgbaston, B15 2TT, United Kingdom

Supporting Information

ABSTRACT: A new peptide sequence (MB1) has been designed which, in the presence of a trivalent lanthanide ion, has been programmed to self-assemble to form a three stranded metallo-coiled coil, Ln(III)(MB1)₃. The binding site has been incorporated into the hydrophobic core using natural amino acids, restricting water access to the lanthanide. The resulting terbium coiled coil displays luminescent properties consistent with a lack of first coordination sphere water molecules. Despite this the gadolinium coiled coil, the first to be reported, displays promising magnetic resonance contrast capabilities.

Magnetic resonance imaging (MRI) is a noninvasive imaging technique routinely employed in medical diagnostics. Commonly paramagnetic agents, such as Gd(III) complexes, are utilized to enhance the image contrast.¹ Factors that are important for optimal performance of these contrast agents include the number of coordinated water molecules, the rate at which they exchange with the bulk water, and the tumbling rate of the complex in solution. However, the majority of Gd(III) complexes used as MRI contrast agents do not display optimal relaxivity, due to their small size and rapid tumbling in solution. Efforts have therefore been directed toward the preparation of macromolecular Gd(III)-based contrast agents. These have included modified dendrimers, nanotubes, polymers, and liposomes, as well as natural biological macromolecules such as proteins and chimeric proteins.^{2–7} The latter are extremely attractive as they offer opportunities to incorporate biomolecular recognition, specificity, and targeting into the design. Nonetheless, drawbacks are associated with their intrinsic complexity, rendering it challenging to correlate Gd(III) coordination chemistry with changes to the primary amino acid sequence, and therefore difficult to redesign optimal Gd(III)–protein structures for use in MRI.

An attractive approach would thus be to employ de novo (from “first principles”) peptide design in order to develop simplified protein folds with which structure–function relationships can be more readily ascertained. Though a range of different structural motifs have been studied, including β -sheets and mixed α/β -motifs, the majority of work has focused on coiled coils, in which multiple α -helices are supercoiled around one another. Metal ion binding sites have been successfully engineered into the interior of these structures, and one can take advantage of various design features to alter the metal ion coordination chemistry.^{8–11} This can include the hydration

state of a coordinated metal ion, a crucial parameter for MRI.^{5,12–14}

Of particular relevance to this work are the reports by Hodges and co-workers on the design of a coiled coil that folds in the presence of Ln(III) by binding to charged residues at the α -helical interface.^{15,16} More recently, Kashiwada and co-workers described the design of a Ln(III) binding site within the hydrophobic core of a coiled coil using γ -carboxy glutamic acid.¹⁷ However, the use of non-natural amino acids such as these (or related derivatives) is expensive and limits their use to peptides that are readily synthesized, making the design of Ln(III) binding sites with natural amino-acids very attractive. Furthermore, in both examples no details were provided concerning the hydration state of the Ln(III) ions, and no reports exist on Gd(III) binding. Ultimately, the opportunity to rationally design a Gd(III) binding site for MRI applications, has not been explored. Our efforts have therefore been directed toward designing a Gd(III) binding site within a de novo designed α -helical coiled coil using natural amino acids and evaluating the Gd(III) coordination chemistry, with the view to investigating the potential of Gd(III)-coiled coils for MRI applications.

In this study, a coiled coil structure has been designed based on the sequence Ac-G(I_aA_bA_cI_dE_eQ_fK_g)_xG-NH₂, which utilizes the heptad (a–g) repeat approach. Isoleucine (Ile, I) residues located in the a and d positions of the heptad generate the hydrophobic core and favor the formation of a three-stranded coiled coil (vide infra).¹⁸ Alanine (Ala, A) residues in the b and c positions are helix inducing, and favorable interhelical salt bridges are formed between glutamate (Glu, E) and lysine (Lys, K) side chains in the e and g positions.¹⁹ The Glu and Lys residues, in addition to the glutamine (Gln, Q) residue in the f position, help solubilize the coiled coil. A rationally designed lanthanide binding site has been introduced in the hydrophobic interior of the coiled coil by replacing two adjacent Ile residues with an asparagine (Asn, N) and aspartate (Asp, D), so as to generate a hard oxygen binding site with which to sequester, for example, Gd(III) or Tb(III) ions that possess similar radii and coordination preferences. A three-stranded coiled coil was selected so that the negative charge of the Asp residues would be neutralized on coordinating the Ln(III) ion. The Asn residue was introduced at the d site in the second heptad (position 12), as d sites have been reported to favor formation of three-stranded coiled coils, whereas its introduction in an a site would encourage the formation of a two-stranded coiled coil.¹⁸ The

Received: August 23, 2013

Published: January 9, 2014



introduction of Asp in the layer directly below (position 16, a site) completes our Ln(III) binding site, which is otherwise flanked by hydrophobic Ile layers. Finally, a tryptophan (Trp, W) was introduced adjacent to the designed metal binding site (in position 14, a f site) as it offers a number of advantages: it absorbs light at 280 nm ($\epsilon_{280} = 5690 \text{ M}^{-1} \text{ cm}^{-1}$), allowing the concentration of the peptide to be readily determined in solution; its emission peak is highly sensitive to its environment; and finally, the Trp indole is capable of sensitizing lanthanide luminescence (vide infra).

The Ln(III) binding site was modeled, and the structure was minimized and subjected to 10.0 ns of molecular dynamics (MD) simulations, see Figure 1. According to this model, the

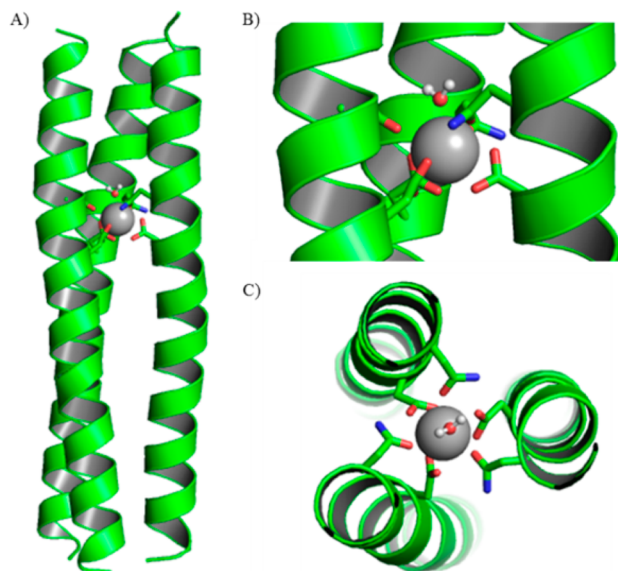


Figure 1. (A) Structure of $\text{Gd}(\text{MB1})_3$ after 10.0 ns of MD simulations, and close-up (B) side-on and (C) top-down views of the $\text{Gd}(\text{III})$ coordination site. Shown are the main chain atoms represented as helical ribbons (green), the Asn and Asp side chains in stick form (oxygen in red and nitrogen in blue), a water molecule in ball-and-stick form, and the $\text{Gd}(\text{III})$ ion as a sphere (gray).

Ln(III) ion is coordinated through three Asp side chains and three carbonyl oxygen atoms from the Asn residues in the layer above, to generate an attractive Ln(III) coordination site. These simulations suggest that a water molecule could coordinate directly to the Ln(III) ion. No significant change was observed between the energy-minimized built structure of the binding site and the equilibrated structure, suggesting a high degree of stability when the ion is bound.

The incorporation of Asn and Asp residues within the hydrophobic core of the coiled coil was anticipated to be highly destabilizing. Thus in an effort to compensate for this, our designed peptide (MB1) contains five heptad repeats ($x = 5$), Ac-G IAAIEQK IAANEWK DAAIEQK IAAIEQK IAAIEQK G-NH₂, as a fifth heptad has previously been reported to stabilize a coiled coil by $\sim 5 \text{ kcal mol}^{-1}$.²⁰ The predicted destabilizing effect of the Ln(III) binding site, was clearly evident in the circular dichroism (CD) spectrum of MB1 in the absence of a metal ion. The low intensity at 222 nm ($\Theta_{222} = -10178 \text{ deg dmol}^{-1} \text{ cm}^2 \text{ res}^{-1}$), which is an indication of the α -helical content, was consistent with a poorly folded peptide (>25%), see Figure 2A. In the absence of Ln(III) the negative charges on the Asp residues repel each other, destabilizing the

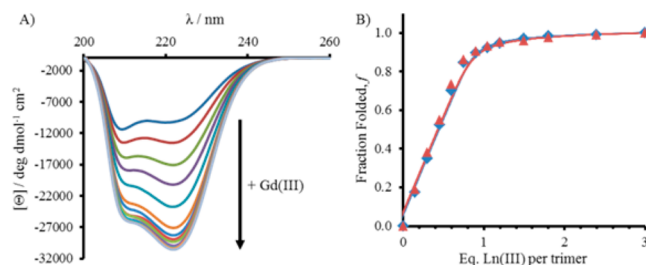


Figure 2. (A) GdCl_3 titration into 100 μM MB1 monomer in 5 mM HEPES buffer pH 7.0 monitored by CD, going from 0 to 100 μM $\text{Gd}(\text{III})$. (B) Plot of normalized fraction folded peptide (based on molar ellipticity at 222 nm) as a function of $\text{Gd}(\text{III})$ (blue diamonds) and $\text{Tb}(\text{III})$ (red triangles) equivalents per trimer. Lines represent best fits using eq 4 (Supporting Information).

coiled coil. However, the intensity of the minima at 222 nm becomes more negative on addition of GdCl_3 into a 30 μM peptide monomer solution in 5 mM HEPES buffer pH 7.0, reaching a plateau after addition of one $\text{Gd}(\text{III})$ per three-stranded coiled coil (see Figure 2B). Under these conditions the CD profile resembled that of a well folded α -helical coiled coil ($\Theta_{222} = -29857 \text{ deg dmol}^{-1} \text{ cm}^2 \text{ res}^{-1}$, ca. 76% folded) consistent with formation of the intended $\text{Gd}(\text{MB1})_3$, see Figure 2A. Mass spectrometry studies are also consistent with the proposed $\text{Gd}(\text{III})(\text{MB1})_3$ complex (see Figure S2A). The sedimentation equilibrium data in the presence of $\text{Gd}(\text{III})$ were best fit to a monomer-to-trimer model (see Figure S3 and Table S1). The CD metal titration data were therefore fit to $1/3 \text{ Ln}(\text{III}) + \text{MB1} \leftrightarrow 1/3 (\text{Ln}(\text{III})\text{MB1})_3$, to yield an association constant ($\log K_a$) of 5.11 ± 0.04 , see Figure 2B. This corresponds to an estimated 86% of the total $\text{Gd}(\text{III})$ complexed to the peptide, at 33 μM GdCl_3 and 100 μM (3 equiv) MB1 (see Figure S4). A related titration of TbCl_3 into a solution of peptide MB1 monitored by CD yields very similar results as for GdCl_3 , resulting in the formation of $\text{Tb}(\text{MB1})_3$ with $\log K_a = 5.03 \pm 0.04$, see Figure 2B. Similar induced folding was observed by CD on addition of $\text{Ce}(\text{III})$, $\text{Nd}(\text{III})$, $\text{Eu}(\text{III})$, $\text{Dy}(\text{III})$, $\text{Er}(\text{III})$, and $\text{Yb}(\text{III})$.

A thermal unfolding experiment of the apo peptide found it to be largely unfolded over the temperature range 20–90 $^\circ\text{C}$; however, a related experiment performed in the presence of $\text{Gd}(\text{III})$, displayed the beginning of a characteristic sigmoidal unfolding curve (see Figure S5). Extrapolation of the data indicates that the T_m is likely to be ca. 60 $^\circ\text{C}$, but importantly the $\text{Gd}(\text{MB1})_3$ complex remains largely folded at biologically relevant temperatures (310 K). Combined, the CD and thermal unfolding data indicate that the $\text{Gd}(\text{III})$ ion behaves like a structural metal which is capable of inducing and stabilizing the correct peptide fold on binding.

We studied the luminescence properties of $\text{Tb}(\text{III})$ in order to obtain insight into the coordination environment around the metal. The Trp indole located at position 14, directly adjacent to the $\text{Tb}(\text{III})$ binding site, can act as a sensitizer for $\text{Tb}(\text{III})$ luminescence. Microliter quantities of a solution of TbCl_3 (1 mM) were added to a solution of MB1 peptide monomer (27 μM) in HEPES buffer pH 7.0 and the $\text{Tb}(\text{III})$ emission monitored between 475 and 700 nm upon excitation at 280 nm (Figure 3A). The characteristic sharp $\text{Tb}(\text{III})$ emission profile with peaks at 490, 545, 585, 620, and 650 nm is obtained, and a plot of the integrated emission intensity over the range 530–560 nm, as a function of $\text{Tb}(\text{III})$ equivalents, shows a sharp increase followed by a plateau which is consistent with

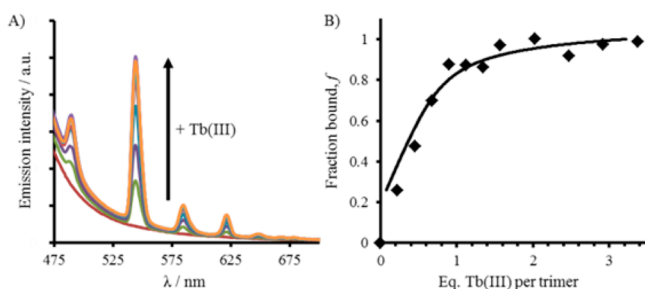


Figure 3. (A) Emission spectra upon titration of Tb(III) into 26.7 μM MB1 monomer in 5 mM HEPES buffer pH 7.0, ranging from 0 (dark red) to 30 μM Tb(III) (orange), $\lambda_{\text{exc}} = 280$ nm. (B) Relative integrated emission intensity as a function of the equivalents of Tb(III) per trimer. Line represents best fit using eq 4 (Supporting Information).

saturation of the binding site with Tb(III) ions (Figure 3B). The saturation curve suggests that a stoichiometry of 1:3 Tb:MB1 exists in agreement with the designed Tb(MB1)₃ formulation, again supported by mass spectrometry (Figure S2B). The data can be fit to yield $\log K_a = 4.96 \pm 0.37$. A comparison of the emission intensity of Tb(MB1)₃ with a solution of TbCl₃ at the same concentration shows a 30-fold enhancement of the Tb(III) emission in the presence of MB1. The emission enhancement is attributed to both coordination to the binding site and sensitization by the Trp unit, as shown by excitation spectroscopy when the Tb(III) luminescence signal is monitored (Figure S6).

Monitoring the Trp emission signal (305–450 nm) upon titration of TbCl₃ into MB1 monomer under the same conditions as above, shows a 30% signal increase compared to the apo-peptide. This is accompanied by a 1 nm blue shift in the UV–vis titration, and a 6% increase in absorption. These results indicate that although there is sensitization from Trp to Tb(III) an apparent decrease of Trp signal is not observed. This is attributed to a change in the environment of the Trp side chain upon complexation of the Tb(III) and folding of the coiled coil.^{21,22}

The large majority of engineered Ln(III) binding sites in proteins are inspired by Ca(II) binding loops.^{23–25} Despite the fact that our Ln(III) binding site did not evolve from a native Ca(II) binding site, we wished to evaluate whether Ca(II) binding would compete or interfere with the intended Ln(III) binding. CD spectra recorded in the absence or presence of 10 mM CaCl₂ were consistent with no substantial change to the solution structure of the peptide either in the absence or presence of Gd(III), see Figure S7. Similarly, Tb(III) luminescence experiments performed in the presence of 10 mM CaCl₂ resulted in no change to the Tb(III) emission signal which would have decreased if Tb(III) was displaced by Ca(II), see Figure S8. Importantly, these experiments demonstrate that our designed peptide displays selectivity toward trivalent lanthanide ions, consistent with the complementary charge of our designed site and their preference for bidentate coordination in confined coordination environments.²⁶

To obtain further information about the Tb(III) coordination environment we studied the luminescence lifetimes of Tb(MB1)₃ in H₂O and D₂O. The luminescence lifetime decays of Tb(MB1)₃ at 545 nm were recorded as 2.05 ms in H₂O and 2.48 ms in D₂O. Applying the Horrocks–Sudnick equation, 0.4 water molecules are estimated to be bound to the Tb(III) ion.²⁷ To correct for the contribution of the outer sphere water

molecules we employed the Parker–Beby equation, which results in 0.1 water molecules being bound to the Tb(III) ion.²⁸ These results infer that although there is some contribution from outer sphere water molecules in quenching Tb(III) luminescence, the contribution from directly coordinated water is minimal. However, these results do not conclusively predict the hydration state of the Gd(III) coiled coil, as it has previously been noted that in some cases the hydration of Gd(III) complexes behaves more like their Eu(III) analogues than their Tb(III) analogues. To make further conclusions on this matter, NMRD experiments are required to determine distances between Gd(III) and water molecules.

It therefore remained for us to evaluate the MRI properties of the resulting Gd(MB1)₃ complex. The longitudinal (T_1) and transverse (T_2) magnetic resonance relaxation times of water protons were monitored in the presence of increasing concentrations of Gd(MB1)₃ and Gd(DOTA) in 10 mM HEPES, pH 7.0, respectively, using CPMG and inversion recovery experiments¹ at 300 MHz (7 T) (Figure S9). These experiments reveal a comparable longitudinal ($r_1 = 6.3 \pm 2.1$ mM⁻¹ s⁻¹) and enhanced transverse ($r_2 = 18.9 \pm 1.5$ mM⁻¹ s⁻¹) relaxivity of Gd(MB1)₃ compared to the widely used contrast agent, Dotarem (GdDOTA) ($r_1 = 4.3 \pm 1.0$ mM⁻¹ s⁻¹; $r_2 = 5.7 \pm 1.8$ mM⁻¹ s⁻¹). Multiple mechanisms exist whereby the relaxation time of bulk water protons can be reduced by a paramagnetic Gd(III). However, the luminescence decay data are inconsistent with a mechanism which involves exchange of a directly coordinated water molecule, as the Gd(III) is buried within the hydrophobic core, restricting water coordination and exchange with the bulk. Therefore the enhancement in relaxivity is likely due to a combination of outer sphere effects and reduced tumbling. Potential outer sphere mechanisms could involve the formation of a hydrogen bonding network between the peptide scaffold and water molecules, aligning these in close proximity to the Gd(III) for sufficient time for the magnetization to be transferred to the water protons. This is similar to a mechanism proposed for the T_2 superparamagnetic iron oxide nanoparticles (SPIONs).²⁹ Additionally, the large number of exchangeable peptide protons in close proximity to the Gd(III) could also be a mechanism by which the relaxation time of bulk water protons is reduced.

T_1 and T_2 maps were recorded of phantom samples containing 100 μM GdCl₃ in 10 mM HEPES buffer pH 7.0. On addition of MB1 and subsequent formation of Gd(MB1)₃, one observes a reduction in the T_2 relaxation time, consistent with a negative contrast agent, see Figure 4. The T_1 maps show a less pronounced change due to the lower longitudinal

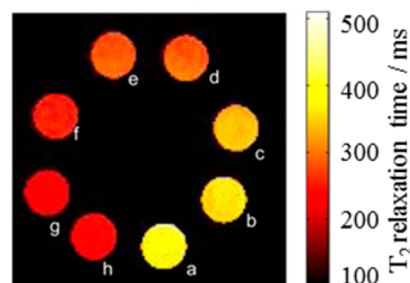


Figure 4. T_2 map of phantom samples containing 100 μM Gd(III) in 10 mM HEPES buffer pH 7.0. Samples a–h contain increasing amounts of (MB1)₃: 0.0 (a), 0.1 (b), 0.2 (c), 0.3 (d), 0.4 (e), 0.6 (f), 0.8 (g), and 1.0 equiv (h).

relaxivity determined for Gd(MB1)₃, see Figure S10. Our efforts are currently directed toward trying to understand the mechanism by which our designed Gd(MB1)₃ alters the relaxation rate of bulk water.

In summary, we report the de novo design of a novel peptide sequence which when in the presence of a trivalent lanthanide ion and under the appropriate conditions is programmed to yield a well folded lanthanide-coiled coil, a model of which has been subjected to 10.0 ns of MD simulations. Both Tb(III) and Gd(III) coiled coils were investigated, the latter representing the first example of its kind to be reported. The Tb(III) complex was studied by luminescence, and the Gd(III) complex has been shown by MRI to display promising T₂ contrast agent capabilities. Notably Ln(III) binding was achieved using natural amino acids and was not based on a native Ca(II) binding site. As a result the designed peptide displayed important selectivity for Ln(III) over Ca(II). By designing the binding site within the hydrophobic core we believe we will be able to control water access to the paramagnetic metal ion in future designs.¹¹ Work is currently being undertaken to enhance the Ln(III) binding constant and to increase the number of first coordination sphere water molecules, so as to yield complexes with improved relaxation efficiency. Importantly, this work has, for the first time, investigated the use of an entirely new class of ligands for Ln(III) ions, with the view to their potential applications as luminescent probes (Tb) and MRI contrast agents (Gd).

■ ASSOCIATED CONTENT

📄 Supporting Information

Materials and methods, additional supplementary characterization including mass spectrometry, sedimentation equilibrium experiments, circular dichroism, luminescence, and NMR data. This material is available free of charge via the Internet at <http://pubs.acs.org>.

■ AUTHOR INFORMATION

Corresponding Author

a.f.a.peacock@bham.ac.uk

Notes

The authors declare no competing financial interest.

■ ACKNOWLEDGMENTS

We thank the School of Chemistry, the EPSRC, and the University of Birmingham for a Ph.D. studentship and for support of this research. D.J.L. and Z.P. thank the EPSRC. Some equipment used was obtained through Birmingham Science City: Innovative Uses for Advanced Materials in the Modern World (West Midlands Centre for Advanced Materials Project 2) and Birmingham Science City Translational Medicine: Experimental Medicine Network of Excellence project, with support from Advantage West Midlands (AWM) and part funded by European Regional Development fund (ERDF).

■ REFERENCES

- (1) Britton, M. M. *Chem. Soc. Rev.* **2010**, *39*, 4036.
- (2) Caravan, P.; Ellison, J. J.; McMurry, T. J.; Lauffer, R. B. *Chem. Rev.* **1999**, *99*, 2293.
- (3) Xu, Q.; Zhu, L.; Yu, M.; Feng, F.; An, L.; Xing, C.; Wang, S. *Polymer* **2010**, *51*, 1336.
- (4) Sitharaman, B.; Kissell, K. R.; Hartman, K. B.; Tran, L. A.; Baikalov, A.; Rusakova, I.; Sun, Y.; Khant, H. A.; Ludtke, S. J.; Chiu,

W.; Laus, S.; Tóth, É.; Helm, L.; Merbach, A. E.; Wilson, L. J. *Chem. Commun.* **2005**, 3915.

(5) Floyd, W. C., III; Klemm, P. J.; Smiles, D. E.; Kohlgruber, A. C.; Pierre, V. C.; Mynar, J. L.; Fréchet, J. M. J.; Raymond, K. N. *J. Am. Chem. Soc.* **2011**, *133*, 2390.

(6) Yang, J. J.; Yang, J.; Wei, L.; Zurkiya, O.; Yang, W.; Li, S.; Zou, J.; Zhou, Y.; Wilkins Maniccia, A. L.; Mao, H.; Zhao, F.; Malchow, R.; Zhao, S.; Johnson, J.; Hu, X.; Krogstad, E.; Liu, Z.-R. *J. Am. Chem. Soc.* **2008**, *130*, 9260.

(7) Caravan, P.; Greenwood, J. M.; Welch, J. T.; Franklin, S. J. *Chem. Commun.* **2003**, 2574.

(8) Kennedy, M. L.; Gibney, B. R. *Curr. Opin. Struct. Biol.* **2001**, *11*, 485.

(9) Pecoraro, V. L.; Peacock, A. F. A.; Iranzo, O.; Łuczowski, M. Understanding the Biological Chemistry of Mercury Using a de novo Protein Design Strategy. In *Bioinorganic Chemistry: Cellular Systems and Synthetic Models*; Long, E., Baldwin, M., Eds.; ACS Symposium Series 1012; American Chemical Society: Washington, DC, 2009; pp 183–197; ISBN: 978-0-8412-6975-0.

(10) Ghosh, D.; Pecoraro, V. L. *Inorg. Chem.* **2004**, *43*, 7902.

(11) Peacock, A. F. A.; Iranzo, O.; Pecoraro, V. L. *Dalton Trans.* **2009**, 2271.

(12) Monera, O. D.; Sönnichsen, F. D.; Hicks, L.; Kay, C. M.; Hodges, R. S. *Protein Eng.* **1996**, *9*, 353.

(13) Lee, K.-H.; Cabello, C.; Hemmingsen, L.; Marsh, E. N. G.; Pecoraro, V. L. *Angew. Chem., Int. Ed.* **2006**, *45*, 2864.

(14) Peacock, A. F. A.; Pecoraro, V. L. In *Cadmium: From Toxicity to Essentiality*; Metal Ions in Life Sciences 11; Sigel, A., Sigel, H., Sigel, R. K. O., Eds.; Springer Science + Business Media B.V.: Dordrecht, 2013; pp 303–337.

(15) Kohn, W. D.; Kay, C. M.; Hodges, R. S. *J. Pept. Res.* **1998**, *51*, 9.

(16) Kohn, W. D.; Kay, C. M.; Sykes, B. D.; Hodges, R. S. *J. Am. Chem. Soc.* **1998**, *120*, 1124.

(17) Kashiwada, A.; Ishida, K.; Matsuda, K. *Bull. Chem. Soc. Jpn.* **2007**, *80*, 2203.

(18) Fletcher, J. M.; Boyle, A. L.; Bruning, M.; Bartlett, G. J.; Vincent, T. L.; Zaccai, N. R.; Armstrong, C. T.; Bromley, E. H. C.; Booth, P. J.; Brady, R. L.; Thomson, A. R.; Woolfson, D. N. *ACS Synth. Biol.* **2012**, *1*, 240.

(19) Pace, C. N.; Scholtz, J. M. *Biophys. J.* **1998**, *75*, 422.

(20) Ghosh, D.; Lee, K.-H.; Demeler, B.; Pecoraro, V. L. *Biochemistry* **2005**, *44*, 10732.

(21) Beechem, J. M.; Brand, L. *Annu. Rev. Biochem.* **1985**, *54*, 43.

(22) Vivian, J. T.; Callis, P. R. *Biophys. J.* **2001**, *80*, 2093.

(23) Allen, K. N.; Imperiali, B. *Curr. Opin. Chem. Biol.* **2010**, *14*, 247.

(24) Kim, Y.; Welch, J. T.; Lindstrom, K. M.; Franklin, S. J. *J. Biol. Inorg. Chem.* **2001**, *6*, 173.

(25) Jain, S.; Welch, J. T.; Horrocks, W. D., Jr.; Franklin, S. J. *Inorg. Chem.* **2003**, *42*, 8098.

(26) Dudev, T.; Lim, C. *Acc. Chem. Res.* **2007**, *40*, 85.

(27) Horrocks, W. D., Jr.; Sudnick, D. R. *Acc. Chem. Res.* **1981**, *14*, 384.

(28) Beeby, A.; Clarkson, I. M.; Dickins, R. S.; Faulkner, S.; Parker, D.; Royle, L.; de Sousa, A. S.; Williams, J. A. G.; Woods, M. *J. Chem. Soc., Perkin Trans. 2* **1999**, 493.

(29) Qin, J.; Laurent, S.; Jo, Y. S.; Roch, A.; Mikhaylova, M.; Bhujwala, Z. M.; Muller, R. N.; Muhammed, M. *Adv. Mater.* **2007**, *19*, 1874.